Shifts from a distant neighboring resonance

M. Horbatsch and E. A. Hessels*
Department of Physics and Astronomy, York University, Toronto, Ontario M3J 1P3, Canada
(Received 13 August 2010; published 24 November 2010)

The line center of a resonance is affected by the presence of neighboring resonances due to quantum interference between the two resonant processes. Such shifts must be accounted for in high-precision measurements but are easily overlooked. In the present work, we develop an analytic formulation for the effect in the simplest case of a three-level atom. The shifts in this model system are large enough to be of concern for precision measurements.

DOI: 10.1103/PhysRevA.82.052519 PACS number(s): 32.70.Jz, 32.80.−t

When an atom has two resonant transitions that are closely spaced in energy, quantum-mechanical interference can cause a variety of effects on the resonances. One of the clearest demonstrations of such interference is the quantum beats phenomenon [1], in which a coherently excited superposition of two neighboring states shows interference between the radiative decay from the two atomic levels. Since radiative decay is a QED process [2], the explanation of interference effects involving this decay must be developed from QED theory [3,4]. For atomic systems, radiative decay is usually treated through density matrices [5–7] and is based upon the essential-state approach [8]. Quantum-mechanical interference in the density-matrix formalism has been derived from QED [9–11]. There are a range of effects predicted due to this interference, including narrowing of spectral lines [12–14], cancellation of spontaneous emission [15], phase control of spontaneous emission [16], and distortions and asymmetries of Lorentzian line shapes [17–23].

In this article, we calculate the shifts of atomic resonances from quantum-mechanical interference due to the presence of a distant neighboring resonance. We study the simplest example (see Fig. 1) of a three-level atom in which a single monochromatic perturbation $V(t) = V_0 \cos(\omega t + \phi)$ is nearly resonant with the $|1\rangle \rightarrow |2\rangle$ transition and far off resonance with the $|1\rangle \rightarrow |3\rangle$ transition. It is assumed that $V_{12} = V_{21}^*$ and $V_{13} = V_{31}^*$ are the only nonzero $V_{ij} = \langle i|V_0|j\rangle$, that states $|2\rangle$ and $|3\rangle$ decay radiatively down to only state $|1\rangle$, and that this radiative decay has the same polarization for both states. We derive analytic formulas for the shift in the $|1\rangle \rightarrow |2\rangle$ resonance and discuss the dependence on the time that the atom interacts with the perturbation, the perturbation amplitude V_0, and the radiative decay rates. In Sec. I, we consider the even simpler two-level problem, where state $|3\rangle$ is excluded. In Sec. II, we show how the presence of state $|3\rangle$ shifts the $|1\rangle \rightarrow |2\rangle$ resonance. In Sec. III, we discuss these shifts for the three-level system, and in Sec. IV, we discuss systems with more than three levels, and, in particular, shifts for the helium triplet states.

I. TWO-LEVEL ATOM

Suppose that state $|3\rangle$ of Fig. 1 is not present and the remaining two-level atom is exposed to a monochromatic perturbation. Within the rotating-wave approximation in which the nonresonant $\exp(-i\omega t - i\phi)$ part of $\cos(\omega t + \phi)$ is ignored, the two-level atom can be described in the density matrix formalism by

$$\dot{\rho}_{22} = -\gamma_2 \rho_{22} - i\frac{\Omega_2}{2}\rho_{12} + i\frac{\Omega_2^*}{2}\rho_{21}, \tag{1a}$$

$$\dot{\rho}_{21} = i\Omega_2 \rho_{22} + \left(i\Delta_2 - \frac{\gamma_2}{2}\right)\rho_{21} - i\frac{\Omega_2}{2}, \tag{1b}$$

where $\Omega_2 = \langle 1|V_0|2\rangle/\hbar$ is the Rabi frequency, Ω_2^* its complex conjugate, $\Delta_2 = \omega - \omega_{21}$ (as shown in Fig. 1), and $\tau_2 = \gamma_2^{-1}$ is the lifetime of state $|2\rangle$. Conservation of probability $\rho_{11} + \rho_{22} = 1$ determines ρ_{11} and $\rho_{12} = \rho_{21}^*$. Combining Eqs. (1a) and (1b) and the complex conjugate of (1b) yields a third-order differential equation for ρ_{22}:

$$\begin{aligned} &4\dddot{\rho}_{22} + 8\gamma_2\ddot{\rho}_{22} + \left(4\Delta_2^2 + 5\gamma_2^2 + 4|\Omega_2|^2\right)\dot{\rho}_{22} \\ &\quad + \left(4\Delta_2^2\gamma_2 + 2|\Omega_2|^2\gamma_2 + \gamma_2^3\right)\rho_{22} = \gamma_2|\Omega_2|^2 . \end{aligned} \tag{2}$$

For an atom that starts in the ground state $|1\rangle$ at $t = 0$, the solution to Eq. (2) at time $t = T$ is

$$\rho_{22} = \rho_{22}^{SS} + e^{-\gamma_B T}[A\sin(vT) - B\cos(vT)] + Ce^{-\gamma_A T}, \tag{3}$$

where

$$\rho_{22}^{SS} = \frac{|\Omega_2|^2}{4\Delta_2^2 + \gamma_2^2 + 2|\Omega_2|^2}, \tag{4a}$$

$$A = \frac{C(\gamma_A - \gamma_B) - \gamma_B \rho_{22}^{SS}}{v}, \tag{4b}$$

$$B = C + \rho_{22}^{SS}, \tag{4c}$$

$$C = \frac{|\Omega_2|^2 - 2\rho_{22}^{SS}\left(\gamma_B^2 + v^2\right)}{2[(\gamma_A - \gamma_B)^2 + v^2]}, \tag{4d}$$

$$\gamma_A = \frac{2}{3}\gamma_2 + \frac{1}{12}\left(\frac{\alpha}{b} - b\right), \tag{4e}$$

$$\gamma_B = \frac{2}{3}\gamma_2 - \frac{1}{24}\left(\frac{\alpha}{b} - b\right), \tag{4f}$$

$$v = \frac{\sqrt{3}}{24}\left(\frac{\alpha}{b} + b\right), \tag{4g}$$

$$b = \sqrt[3]{\beta + \sqrt{\alpha^3 + \beta^2}}, \tag{4h}$$

$$\alpha = 48\left(\Delta_2^2 + |\Omega_2|^2 - \frac{1}{12}\gamma_2^2\right), \tag{4i}$$

$$\beta = 8\gamma_2\left(18|\Omega_2|^2 - 36\Delta_2^2 - \gamma_2^2\right). \tag{4j}$$

Note that since ρ_{22} (the population of state $|2\rangle$) depends only on the square of Δ_2, the line shape is perfectly symmetric about

*hessels@yorku.ca

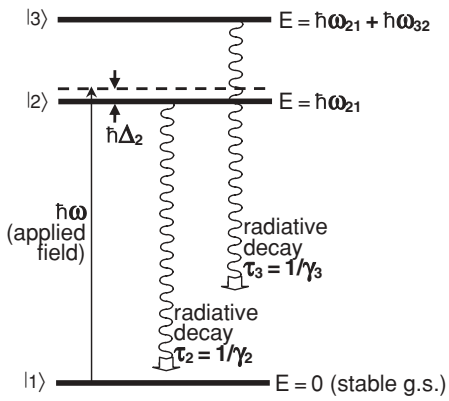

FIG. 1. The three-level atom. A single monochromatic applied field is nearly in resonance with the $|1\rangle \rightarrow |2\rangle$ transition but far off resonance with the $|1\rangle \rightarrow |3\rangle$ transition. Both state $|2\rangle$ and state $|3\rangle$ radiatively decay down to state $|1\rangle$. We consider the case in which the entire population starts in state $|1\rangle$ at $t = 0$ and find the population of state $|2\rangle$ at time $t = T$. Interference effects between states $|2\rangle$ and $|3\rangle$ cause shifts in the resonant frequency for driving population to state $|2\rangle$.

$\Delta_2 = 0$, and thus the line shape is exactly centered at $\omega = \omega_{21}$. For long interaction time T, Eq. (3) reduces to the steady-state solution $\rho_{22} \rightarrow \rho_{22}^{SS}$ [Eq. (4a)], which recovers the familiar power-broadened Lorentzian line shape. For small $\gamma_2 T$, the line shape reduces to the well-known

$$\rho_{22} \rightarrow |\Omega_2|^2 \frac{\sin^2\left[\sqrt{\Delta_2^2 + |\Omega_2|^2}(T/2)\right]}{\Delta_2^2 + |\Omega_2|^2}, \tag{5}$$

which further reduces to

$$\rho_{22} \rightarrow |\Omega_2|^2 \frac{\sin^2\left[\Delta_2(T/2)\right]}{\Delta_2^2}, \tag{6}$$

in the perturbative regime in which T and Ω_2 are sufficiently small so that ρ_{22} is much smaller than unity. The more general perturbative result (for the case in which $\gamma_2 T$ is not necessarily small) is

$$\rho_{22} \rightarrow \frac{|\Omega_2|^2[1 + e^{-\gamma_2 T} - 2e^{-\gamma_2 \frac{T}{2}} \cos(\Delta_2 T)]}{4\Delta_2^2 + \gamma_2^2}. \tag{7}$$

For intermediate times, when the perturbative solution is no longer valid and the steady-state regime is not yet reached, the line shape Eq. (3) is, in general, more complicated.

Figure 2 shows the half-width-at-half-maximum (HWHM) points for a range of parameters Ω_2, γ_2, and T. Note that the widths obtained from Eq. (3) agree with those from Eqs. (7), (5), and (4a) in their respective ranges of validity. The variable b of Eq. (4a) is real for most of parameter space, including the full range shown in Fig. 2. When b is real, all of the quantities in Eqs. (3) and (4) are real, but Eqs. (3) and (4) are correct even when b is complex.

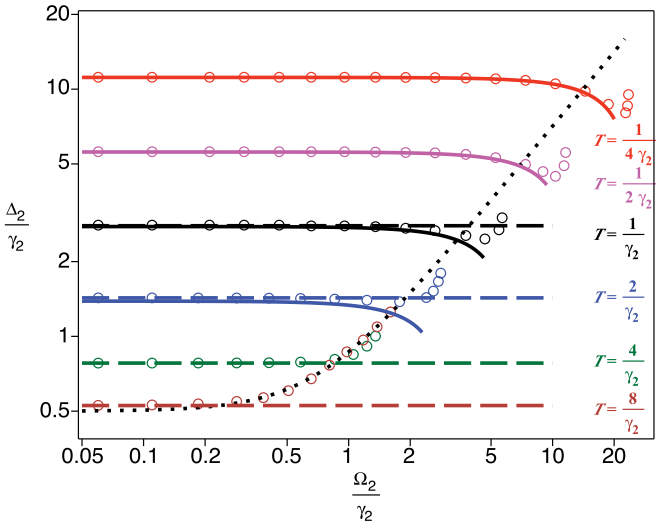

FIG. 2. (Color online) HWHM for the two-level line shape. The circles represent the HWHM for the exact line shape of Eq. (3). These are in good agreement with the widths of Eq. (7) (dashed line) for sufficiently small T and Ω_2, where the perturbative result should be valid. For small $\gamma_2 T$, the width of Eq. (5) (solid lines) agrees with Eq. (3) to larger Ω_2. For large T, the width of Eq. (3) is well approximated by the steady-state solution of Eq. (4a) (dotted line).

II. THREE-LEVEL ATOM

When we consider the full three-level atom of Fig. 1, Eq. (1) expands to [9,10]

$$\dot{\rho}_{22} = -\gamma_2\rho_{22} - i\frac{\Omega_2}{2}\rho_{12} + i\frac{\Omega_2^*}{2}\rho_{21} - \frac{\gamma_{23}}{2}\rho_{23} - \frac{\gamma_{23}}{2}\rho_{32}, \tag{8a}$$

$$\dot{\rho}_{21} = i\Omega_2\rho_{22} + \left(i\Delta_2 - \frac{\gamma_2}{2}\right)\rho_{21} + i\frac{\Omega_3}{2}\rho_{23} - \frac{\gamma_{23}}{2}\rho_{31} + i\frac{\Omega_2}{2}\rho_{33} - i\frac{\Omega_2}{2}, \tag{8b}$$

$$\dot{\rho}_{31} = i\frac{\Omega_3}{2}\rho_{22} + i\Omega_3\rho_{33} - \frac{\gamma_{23}}{2}\rho_{21} + \left[i(\Delta_2 - \omega_{32}) - \frac{\gamma_3}{2}\right]\rho_{31} + i\frac{\Omega_2}{2}\rho_{32} - i\frac{\Omega_3}{2}, \tag{8c}$$

$$\dot{\rho}_{23} = -\frac{\gamma_{23}}{2}\rho_{22} - \frac{\gamma_{23}}{2}\rho_{33} - i\frac{\Omega_2}{2}\rho_{13} + \left(i\omega_{32} - \frac{\gamma_2 + \gamma_3}{2}\right)\rho_{23} + i\frac{\Omega_3^*}{2}\rho_{21}, \tag{8d}$$

$$\dot{\rho}_{33} = -\gamma_3\rho_{33} + i\frac{\Omega_3^*}{2}\rho_{31} - \frac{\gamma_{23}}{2}\rho_{32} - i\frac{\Omega_3}{2}\rho_{13} - \frac{\gamma_{23}}{2}\rho_{23}. \tag{8e}$$

The radiative decay terms in these density matrix equations have been shown to follow from QED [9,10]. The effects of small QED frequency shifts (Lamb shifts) have been neglected, as in [9] and [10]. Equations (8a)–(8e) have been used extensively to describe a wide variety of effects in multilevel systems [12–16,24,25]. In Eq. (8), $\Omega_3 = \langle 1|V_0|3\rangle/\hbar$ and $\tau_3 = \gamma_3^{-1}$ is the lifetime of state $|3\rangle$. The appearance of $\gamma_{23} = (\gamma_2\gamma_3)^{1/2}$ in Eq. (8) indicates the coherence of radiative decay from states $|2\rangle$ and $|3\rangle$. This coherence is possible because the radiation from the decay of these two states has the same polarization. The other components of ρ are

obtained from the complex conjugates of these equations and from conservation of probability for this closed system: $\rho_{11}+\rho_{22}+\rho_{33}=1$.

We wish to solve Eq. (8) in the regime where the two resonances are not overlapping. In our case (Fig. 1), the driving frequency ω is nearly resonant with the $|1\rangle \rightarrow |2\rangle$ transition but far off resonance with the $|1\rangle \rightarrow |3\rangle$ transition, and thus state $|3\rangle$ causes a small perturbation to the line shape of Eq. (3). If the two resonances are sufficiently separated in frequency to not overlap, then $\rho_{33} \ll \rho_{22}$. To proceed, we introduce a small perturbation parameter η, such that ρ_{33} is of order η^2 smaller than ρ_{22}. In terms of this parameter η, the dominant components of the density matrix are ρ_{11}, ρ_{12}, ρ_{21}, and ρ_{22}, whereas ρ_{13}, ρ_{31}, ρ_{23}, and ρ_{32} are a factor of η smaller than these dominant terms, and ρ_{33} is a factor of η^2 smaller. In order to ensure this ordering, it is necessary that Ω_2, Ω_3, γ_2, γ_3, Δ_2, and $2\pi/T$ all be much smaller (by one order in η) than ω_{32}.

Taking a linear combination of Eq. (8a), Eq. (8d), and its complex conjugate allows one to eliminate the ρ_{23} and ρ_{32} terms in Eq. (8a) to the lowest order in η. Keeping only the terms up to first order in η leads to

$$\dot{\rho}_{22} = -\gamma_2\rho_{22} - i\frac{\Omega_2'}{2}\rho_{12} + i\frac{\Omega_2'^*}{2}\rho_{21}, \tag{9}$$

where

$$\Omega_2' = \Omega_2 - i\frac{\gamma_{23}\Omega_3}{2\omega_{32}}. \tag{10}$$

Similarly, if one takes a linear combination of Eqs. (8b), (8c), and (8d), one can eliminate the ρ_{23} and ρ_{31} terms in Eq. (8b) to first order in η to obtain

$$\dot{\rho}_{21} = i\Omega_2\rho_{22} + \left(i\Delta_2' - \frac{\gamma_2}{2}\right)\rho_{21} - i\frac{\Omega_2'}{2}, \tag{11}$$

where

$$\Delta_2' = \Delta_2 - \frac{\gamma_{23}^2 + |\Omega_3|^2}{4\omega_{32}}. \tag{12}$$

Equations (9) through (12) are complete to first order in η.

From the similarity of Eqs. (9) and (11) to Eqs. (1a) and (1b), one can write the expression for ρ_{22}', the probability of being in state $|2\rangle$ at a time T (including the effects of the presence of the off-resonant state $|3\rangle$), by substituting Δ_2 with Δ_2' in Eqs. (3) and (4), as well as substituting Ω_2' for some instances of Ω_2. The result (correct to order η) is

$$\rho_{22}' = \rho_{22}^{SS'} + e^{-\gamma_B' T}[A'\sin(v'T) - B'\cos(v'T)] + C'e^{-\gamma_A' T}, \tag{13}$$

where

$$\rho_{22}^{SS'} = \frac{|\Omega_2|^2}{4\Delta_2'^2 + \gamma_2^2 + 2|\Omega_2|^2 + 2\epsilon\Delta_2'}, \tag{14a}$$

$$A' = \frac{C'(\gamma_A' - \gamma_B') - \gamma_B'\rho_{22}^{SS'}}{v'}, \tag{14b}$$

$$B' = C' + \rho_{22}^{SS'}, \tag{14c}$$

$$C' = \frac{|\Omega_2|^2 - 2\rho_{22}^{SS'}(\gamma'^2_B + v'^2)}{2[(\gamma_A' - \gamma_B')^2 + v'^2]}, \tag{14d}$$

$$\gamma_A' = \frac{2}{3}\gamma_2 + \frac{1}{12}\left(\frac{\alpha'}{b'} - b'\right), \tag{14e}$$

$$\gamma_B' = \frac{2}{3}\gamma_2 - \frac{1}{24}\left(\frac{\alpha'}{b'} - b'\right), \tag{14f}$$

$$v' = \frac{\sqrt{3}}{24}\left(\frac{\alpha'}{b'} + b'\right), \tag{14g}$$

$$b' = \sqrt[3]{\beta' + \sqrt{\alpha'^3 + \beta'^2}}, \tag{14h}$$

$$\alpha' = 48\left(\Delta_2'^2 + |\Omega_2|^2 - \frac{1}{12}\gamma_2^2\right), \tag{14i}$$

$$\beta' = 8\gamma_2\left(18|\Omega_2|^2 - 36\Delta_2'^2 - \gamma_2^2 - 54\epsilon\Delta_2'\right). \tag{14j}$$

Equations (13) and (14) differ from Eqs. (3) and (4) only by the shift in Δ_2' [Eq. (12)] that is proportional to ω_{32}^{-1} (i.e., first-order in the parameter η) and by the small parameter

$$\epsilon = \frac{\gamma_{23}|\Omega_2||\Omega_3|}{\gamma_2\omega_{32}}, \tag{15}$$

which is of the same order in η. Unlike Eq. (3), the line shape of Eq. (13) is shifted from $\omega = \omega_{21}$ both due to the shift in Δ_2' and due to the terms proportional to ϵ that are linear in Δ_2'.

For long interaction times, $\rho_{22}' \rightarrow \rho_{22}^{SS'}$, which can be re-expressed (to first order in η) as

$$\rho_{22}' \rightarrow \frac{|\Omega_2|^2}{4(\Delta_2' + \epsilon/4)^2 + \gamma_2^2 + 2|\Omega_2|^2}. \tag{16}$$

This is a Lorentzian with the same width as Eq. (4a), but shifted by

$$\mathcal{S}_\infty = \frac{\gamma_{23}^2 + |\Omega_3|^2 - (\gamma_{23}/\gamma_2)|\Omega_2||\Omega_3|}{4\omega_{32}}. \tag{17}$$

The $\gamma_{23}^2/4\omega_{32}$ part of this shift in the Lorentzian line shape was previously obtained in a Compton scattering calculation [18].

For small $\gamma_2 T$, Eq. (13) reduces to

$$\rho_{22}' \rightarrow |\Omega_2|^2\frac{\sin^2\left[\sqrt{\Delta_2'^2 + |\Omega_2|^2}(T/2)\right]}{\Delta_2'^2 + |\Omega_2|^2}, \tag{18}$$

which is shifted from $\Delta_2 = 0$ by

$$\mathcal{S}_0 = \frac{\gamma_{23}^2 + |\Omega_3|^2}{4\omega_{32}}. \tag{19}$$

In the perturbative regime (T and Ω_2 sufficiently small), one obtains

$$\rho_{22}' \rightarrow \frac{|\Omega_2|^2[1 + e^{-\gamma_2 T} - 2e^{-\gamma_2\frac{T}{2}}\cos(\Delta_2' T)]}{4\Delta_2'^2 + \gamma_2^2}, \tag{20}$$

which is also shifted by $\mathcal{S}_0$.

Note that even though Eqs. (16), (18), and (20) are shifted by $\mathcal{S}_\infty$, $\mathcal{S}_0$, and $\mathcal{S}_0$, respectively, they still exhibit exactly the same line shapes as the two-level line shapes of Eqs. (4a), (5), and (7). That is, to first order in η, the lines are shifted but not otherwise broadened or distorted.

For small T, there is a linear correction to the shift $\mathcal{S}_0$:

$$\mathcal{S}_{T\approx 0} = \mathcal{S}_0 - \frac{\gamma_{23}|\Omega_2||\Omega_3|}{20\,\omega_{32}}T + O(T^3). \tag{21}$$

Note that in both the limits of small T [Eq. (21)] and large T [Eq. (17)] the shift of the resonant line center depends on

γ_{23}, which results from the quantum-mechanical interference of the radiative decay.

For the three-level system under consideration, since the same matrix elements are present in the radiative decay rates (γ_2 and γ_3) as are present in the Rabi frequencies (Ω_2 and Ω_3), γ_3 is related to γ_2 by

$$\gamma_3 = \gamma_2 \frac{|\Omega_3|^2}{|\Omega_2|^2} \frac{(\omega_{21}+\omega_{32})^3}{\omega_{21}^3}, \tag{22}$$

where the energy differences $\hbar\omega_{ij}$ are shown in Fig. 1. Using this relationship and $\gamma_{23}^2 = \gamma_2\gamma_3$, Eq. (21) becomes

$$\mathcal{S}_{T\approx 0} = \frac{\gamma_{23}^2 + |\Omega_3|^2\{1-(\gamma_2 T/5)[(\omega_{21}+\omega_{32})/\omega_{21}]^{3/2}\}}{4\omega_{32}}, \tag{23}$$

and Eq. (17) becomes

$$\mathcal{S}_{\infty} = \frac{\gamma_{23}^2 + |\Omega_3|^2\{1-[(\omega_{21}+\omega_{32})/\omega_{21}]^{3/2}\}}{4\omega_{32}}. \tag{24}$$

Equations (23) and (24) respectively are the short- and long-T limits of the more general shift

$$\mathcal{S} = \frac{\gamma_{23}^2 + |\Omega_3|^2\{1-f(\Omega_2/\gamma_2,\gamma_2 T)[(\omega_{21}+\omega_{32})/\omega_{21}]^{3/2}\}}{4\omega_{32}}, \tag{25}$$

where the factor f (which depends only on the dimensionless quantities Ω_2/γ_2 and $\gamma_2 T$) determines the amount by which the $|\Omega_3|^2$ shift is suppressed. The factor f is shown in Fig. 3; it grows linearly from zero for small T (as $\gamma_2 T/5$), indicating that the $|\Omega_3|^2$ shift is minimally suppressed for short interaction times T. For long interaction times, the $|\Omega_3|^2$ shift is maximally suppressed.

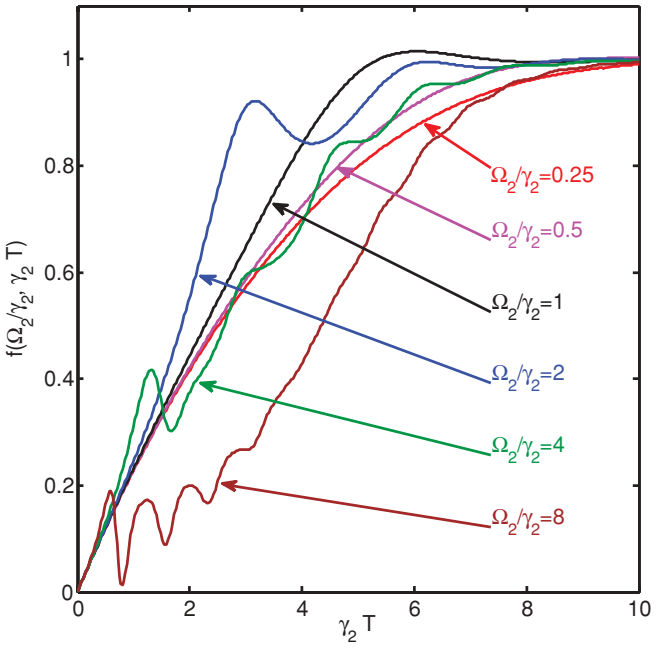

FIG. 3. (Color online) The factor f of Eq. (25) that determines the shift of the $|1\rangle \rightarrow |2\rangle$ transition due to the presence of state $|3\rangle$. The line shifts are obtained by least-squares fits of the three-level line shape of Eq. (13) to the symmetric two-level line shape of Eq. (3) with the center Δ_2 floating in the fit. Note that f starts at zero at $T = 0$ and grows linearly as $\gamma_2 T/5$ as predicted by Eq. (23) and that it reaches unity for large T, as predicted by Eq. (24).

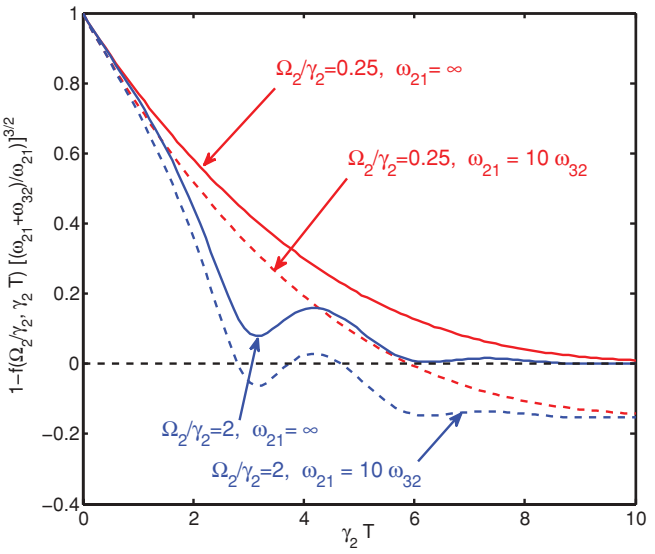

FIG. 4. (Color online) Multiplicative factor for the ac Stark shift. The figure shows that the ac Stark shift must be multiplied by a factor that depends on Rabi frequency Ω_2, on the lifetime γ_2^{-1}, on the interaction time T, and on the ratio of the energy separations: ω_{21}/ω_{32}. For long interaction times T, the shift goes to zero for $\omega_{21}/\omega_{32} = \infty$ and changes sign for finite ω_{21}/ω_{32}.

III. DISCUSSION OF THE SHIFTS

The $|\Omega_3|^2/4\omega_{32}$ term of Eq. (25) is proportional to the amplitude squared (V_0^2) of the monochromatic perturbation (and therefore the intensity of the electromagnetic wave that produces the perturbation). For electric dipole transitions, this is just the usual ac Stark shift. Our result shows that for the model three-level system, this shift must be multiplied by a factor that depends on Ω_2/γ_2, $\gamma_2 T$ and on the ratio $(\omega_{21}+\omega_{32})/\omega_{21}$. Figure 4 shows some examples of the factor by which the ac shift must be multiplied for a variety of these parameters. For the case of $\omega_{32} \ll \omega_{21}$ (two nearby states well above the ground state), this factor is just $1-f$ (where f is shown in Fig. 3). In this case, the ac shift goes from being completely present for short interaction times to being completely suppressed at long interaction times. Thus, we obtain the surprising result that, for a three-level atom, the power-dependent shift can be entirely suppressed in the steady state. For the case of ω_{32} being non-negligible compared to ω_{21}, the shift is still present in its entirety for small interaction times T but changes sign for longer T.

The first part of Eq. (25) is proportional to $\gamma_{23}^2 = \gamma_2\gamma_3$. Since this shift is independent of the intensity of the electromagnetic wave driving the transition, it must be explicitly corrected for in precision measurements, even after extrapolating to zero intensity. When performing precision measurements, this shift is significant even for quite distant neighboring resonances. If the precision measurement has an accuracy of one part in N of the natural linewidth (where N ranges from 500 to 5,000 for many precision measurements), a neighboring

resonance within N natural linewidths of the resonance leads to a significant shift. If γ_3 is greater than γ_2, an even further neighboring resonance ($\frac{\gamma_3}{\gamma_2}N$ natural linewidths away) still leads to a significant shift.

Often for precision measurements, neighboring resonances are simultaneously fit to overlapping Lorentzian line shapes. The overlap of two Lorentzians does lead to a shift that is properly accounted for by such a fit, but this overlap term is of order η^2 and is therefore much smaller than the shift due to quantum-mechanical interference that is discussed here, which is of order η. This $O(\eta)$ shift is not accounted for by the fit to two Lorentzians and must be accounted for separately.

IV. SYSTEMS WITH MORE THAN THREE LEVELS

For more complicated systems with multiple, nearly degenerate ground states, the situation will be more complicated, since such systems exhibit effects such as optical pumping and dark states. These effects will allow population to accumulate into states that no longer interact with the driving field. In these more complicated systems, the shifts are expected to be modified. Additionally, different types of experiments (for example, experiments that determine resonant frequencies from absorption, from fluorescence, or from redistribution of populations) are also expected to give modified shifts. In each of these cases, the shifts can be obtained by numerically solving an expanded form [10] of density-matrix equations of Eq. (8). Such numerical calculations can also model any possible effects of the variation in amplitude of the applied field during the time T. Further investigation will be necessary to characterize the shifts for such multilevel systems. The current work gives the scale for these interference shifts by obtaining simple analytic results for the three-level system of a resonance with a single distant neighboring resonance.

As a simple example of a more complicated system, we consider the lowest-lying triplet states of helium, as shown in Fig. 5. The figure shows the $2\,^3S_1$ and $2\,^3P_J$ states in the presence of a dc magnetic field that lifts the degeneracy of the m_J states. In order to consider a system similar to the three-level system discussed in Sec. II, we assume that optical pumping has been used so that only the $2\,^3S_1\ m_J = 1$ state is

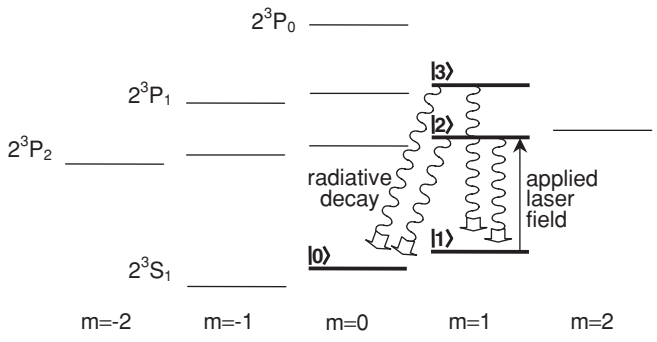

FIG. 5. The $2\,^3S_1$ and $2\,^3P_J$ states of atomic helium in the presence of a dc magnetic field. The population is initially pumped to the $|1\rangle$ state. A laser field polarized in the direction of the magnetic field is nearly in resonance with the $|1\rangle \rightarrow |2\rangle$ transition. The off-resonant $|1\rangle \rightarrow |3\rangle$ transition causes a shift. Both states $|2\rangle$ and $|3\rangle$ decay with equal branching ratios to the $|1\rangle$ and $|0\rangle$ states.

populated, and we designate this as state $|1\rangle$ in Fig. 5. Laser light that is linearly polarized along the direction of the dc magnetic field allows transitions from $|1\rangle$ to only the $2\,^3P_2$ $m_J = 1$ and $2\,^3P_1$ $m_J = 1$ states. If the laser light is nearly resonant with the $2\,^3P_2$ $m_J = 1$ state (designated as $|2\rangle$ in Fig. 5), the $|1\rangle \rightarrow |2\rangle$ resonance line center is shifted by the off-resonant $2\,^3P_1$ $m_J = 1$ state (designated by $|3\rangle$ in Fig. 5). The system is identical to that discussed in Sec. II, except that here states $|2\rangle$ and $|3\rangle$ can also decay down to the $2\,^3S_1\ m_J = 0$ state (designated by $|0\rangle$ in Fig. 5).

For this system and for small T, the shift of the $|1\rangle \rightarrow |2\rangle$ resonance line center (as obtained by measuring the population of state $|2\rangle$ at time T) is still given by Eq. (19), where for this case $\omega_{32}/2\pi = 2.29$ GHz and $\gamma_{23}^2 = \gamma_{2\rightarrow1}\gamma_{3\rightarrow1}$, with $\gamma_{2\rightarrow1}$ being the partial decay rate from state $|2\rangle$ to state $|1\rangle$. Specifically, $\gamma_{2\rightarrow1} = \gamma_{3\rightarrow1} = \frac{1}{2}\ \tau^{-1}$, where $\tau = 98$ ns is the $2\,^3P$ lifetime and $\frac{1}{2}$ is the branching ratio to state $|1\rangle$. The resulting shift (after extrapolating to zero power) is $\Delta f = S_0/2\pi = 72$ Hz. Current measurements of the $2\,^3P$ fine structure are at accuracies of a few hundred hertz [26–28], and thus shifts of the type mentioned here need to be carefully considered for such measurements. In order to obtain a determination of the fine-structure constant to an accuracy of 10^{-9} or better, measurements of the $2\,^3P$ structure to an accuracy of 60 Hz or better must be compared to precise QED calculations of the fine structure [29], and the interference shifts discussed here will again have to be carefully considered.

The ac Stark shift [the $|\Omega_3|^2$ term of Eq. (19)] for the system of Fig. 5 reduces with T, as was the case for the simple three-level system discussed in Sec. III. However, the additional decay channel to state $|0\rangle$ causes the population to be lost to the $|0\rangle$ state. The result is that the population in the $|2\rangle$ state decreases quickly with T, and only measurements of the population of state $|2\rangle$ at not too large values of T become practical.

V. CONCLUSIONS

In the present work, we calculate shifts due to quantum-mechanical interference between a resonance and a distant neighboring resonance using the density-matrix equations for a three-level system. We obtain an interference shift that scales as $1/\omega_{32}$ for all interaction times T (from short pulses to the steady-state regime) and for all intensities of the driving field. The ac Stark shift is obtained naturally from solving the density matrix equations; however, somewhat unexpectedly we find a significant change in the ac shift when moving from the short-T to the steady-state regime.

The present work shows shifts that are still present when extrapolating to zero power, that are not accounted for by a simple fit to overlapping line shapes, and that lead (to first order) to line shapes that are shifted but not otherwise distorted. All three of these properties make the shifts easy to overlook in precision measurements of resonant line centers.

For systems with more than three levels, the calculations will in general be more complicated and will be discussed in more detail in a future publication. Even for these more complicated systems, the present calculation still gives the scale for the interference shifts.

[1] S. Haroche, *Topics in Applied Physics*, edited by K. Shimoda (Springer Verlag, Berlin, 1976), Vol. 13, Chap. 7, pp. 253–313.
[2] J. R. Ackerhalt and J. H. Eberly, Phys. Rev. D **10**, 3350 (1974).
[3] R. M. Herman, H. Grotch, R. Kornblith, and J. H. Eberly, Phys. Rev. A **11**, 1389 (1975).
[4] P. W. Milonni, Phys. Rep. **25**, 1 (1976).
[5] L. D. Landau, Z. Phys. **45**, 430 (1927).
[6] C. Cohen-Tannoudji and S. Reynaud, J. Phys. B **10**, 345 (1977).
[7] C. Cohen-Tannoudji, S. Reynaud, R. K. Bullough, and J. M. Vaughan, Phil. Trans. R. Soc. A **293**, 223 (1979).
[8] V. Weisskopf and E. Wigner, Z. Phys. **63**, 54 (1930).
[9] D. A. Cardimona, M. G. Raymer, and C. R. Stroud Jr, J. Phys. B **15**, 55 (1982).
[10] D. A. Cardimona and C. R. Stroud, Phys. Rev. A **27**, 2456 (1983).
[11] Z. Ficek and S. Swain, *Quantum Interference and Coherence* (Springer-Verlag, Berlin, 2005).
[12] P. Zhou and S. Swain, Phys. Rev. Lett. **77**, 3995 (1996).
[13] C. H. Keitel, Phys. Rev. Lett. **83**, 1307 (1999).
[14] K. T. Kapale, M. O. Scully, S.-Y. Zhu, and M. S. Zubairy, Phys. Rev. A **67**, 023804 (2003).
[15] S.-Y. Zhu and M. O. Scully, Phys. Rev. Lett. **76**, 388 (1996).
[16] E. Paspalakis and P. L. Knight, Phys. Rev. Lett. **81**, 293 (1998).
[17] F. Low, Phys. Rev. **88**, 53 (1952).
[18] L. N. Labzowsky, D. A. Solovyev, G. Plunien, and G. Soff, Phys. Rev. Lett. **87**, 143003 (2001).
[19] L. Labzowsky and D. Solovyev, J. Phys. B **37**, 3271 (2004).
[20] S. G. Karshenboim and V. G. Ivanov, Astron. Lett. **34**, 289 (2008).
[21] O. Andreev, L. Labzowsky, G. Plunien, and D. A. Solovyev, Phys. Rep. **455**, 135 (2008).
[22] L. Labzowsky, G. Schedrin, D. Solovyev, E. Chernovskaya, G. Plunien, and S. Karshenboim, Phys. Rev. A **79**, 052506 (2009).
[23] T. Bergeman, J. Chem. Phys. **61**, 4515 (1974).
[24] R. J. Cook, Phys. Rev. A **29**, 1583 (1984).
[25] M. Artoni and A. Bambini, J. Phys. B **31**, 4501 (1998).
[26] M. Smiciklas and D. Shiner, Phys. Rev. Lett. **105**, 123001 (2010).
[27] J. S. Borbely, M. C. George, L. D. Lombardi, M. Weel, D. W. Fitzakerley, and E. A. Hessels, Phys. Rev. A **79**, 060503 (2009).
[28] T. Zelevinsky, D. Farkas, and G. Gabrielse, Phys. Rev. Lett. **95**, 203001 (2005).
[29] K. Pachucki and V. A. Yerokhin, Phys. Rev. Lett. **104**, 070403 (2010).